 CMC, vol.19, no.2, pp.135-154, 2010

Fracture Analysis of Concrete Structural Components Accounting for Tension Softening Effect

A. Rama Chandra Murthy[1,2], G.S. Palani[1], Nagesh R. Iyer[1]
B.K. Raghu Prasad[3], M Srinivasa Pavan[1] and Smitha Gopinath[1]

Abstract: This paper presents methodologies for fracture analysis of concrete structural components with and without considering tension softening effect. Stress intensity factor (SIF) is computed by using analytical approach and finite element analysis. In the analytical approach, SIF accounting for tension softening effect has been obtained as the difference of SIF obtained using linear elastic fracture mechanics (LEFM) principles and SIF due to closing pressure. Superposition principle has been used by accounting for non-linearity in incremental form. SIF due to crack closing force applied on the effective crack face inside the process zone has been computed using Green's function approach. In finite element analysis, the domain integral method has been used for computation of SIF. The domain integral method is used to calculate the strain energy release rate and SIF when a crack grows. Numerical studies have been conducted on notched 3-point bending concrete specimen with and without considering the cohesive stresses. It is observed from the studies that SIF obtained from the finite element analysis with and without considering the cohesive stresses is in good agreement with the corresponding analytical value. The effect of cohesive stress on SIF decreases with increase of crack length. Further, studies have been conducted on geometrically similar structures and observed that (i) the effect of cohesive stress on SIF is significant with increase of load for a particular crack length and (iii) SIF values decreases with increase of tensile strength for a particular crack length and load.

Keywords: Concrete fracture, fatigue, tension softening, domain integral method, stress intensity factor.

[1] CSIR, Structural Engineering Research Centre, CSIR Campus, Taramani, Chennai, India, 600 113
[2] murthyarc@sercm.org, archandum@yahoo.com, Fax: 91-44-22541508
[3] Civil Engg. Dept., Indian Institute of Science, Bangalore

1 Introduction

Concrete is a widely used material that is required to withstand a large number of cycles of repeated loading in structures such as highways, airports, bridges and offshore structures. The present state-of-the-art of designing such structures against the fatigue mode of distress is largely empirical based on experience. As long as the designer is dealing with structures made of similar to those for which the relationships were derived, the performance can be reasonably well predicted. However, as conditions change, a need exists for a rational approach. Concrete contains numerous flaws, such as holes or air pockets, precracked aggregates, lack of bond between aggregate and matrix, etc., from which cracks may originate. While the shape of the crack is likely to be highly irregular, it is expected that the irregularities will be smoothed out and the cracks will grow in a slow manner to a simple shape along which the stress intensity factor (SIF) is nearly uniform. Fracture mechanics is a rapidly developing field that has great potential for application to concrete structural design.

The fracture behavior of concrete is greatly influenced by the fracture process zone (FPZ). In concrete and rock fracture, the plastic flow is next to nonexistent and the nonlinear zone is almost entirely mobilised by FPZ. Such materials are now commonly called quasi-brittle. The variation of FPZ along the structure thickness or width is usually neglected. The inelastic fracture response due to the presence of FPZ may then be taken into account by a cohesive pressure acting on the crack faces. (Figure 1) shows FPZ in brittle-ductile materials and quasi-brittle materials6. To model this behavior using discrete crack fracture mechanics, it is assumed that an initial crack begins to propagate at the proportional limit f_y and continues to propagate in a stable manner until the peak stress. When the crack extends in concrete, new crack surfaces are formed along the path of the initial crack tip. The newly formed crack surfaces may be in contact and this leads to toughening mechanisms in FPZ such as aggregate bridging. Further, they may continue to sustain some normal tensile stress that is characterized by a material tensile stress-separation relationship.

The first application of fracture mechanics to concrete was made by Kaplan [1961] using linear elastic fracture mechanics (LEFM) principles. Barenblatt [1959] and Dugdale [1960] made the first attempt to include the cohesive forces in the crack tip region within the limits of elasticity theory. Barenblatt [1959] assumed that cohesive forces act in a small zone near the crack ends such that the faces close smoothly. The distribution of these forces is generally unknown. For Dugdale model [1960], the distribution of the closing forces is known and constant according to an elastic-perfectly plastic material. A major advance in concrete fracture was made by Hillerborg et al. [1976], which includes the tension softening process zone

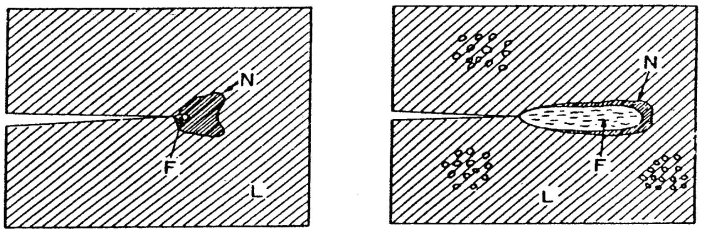

a) Brittle- Ductile (Metals) **b) Quasi-brittle (concrete)**

Figure 1: FPZ in ductile and brittle materials

through a fictitious crack ahead of the pre-existing crack whose lips are acted upon by closing forces such that there is no stress concentration at the tip of this extended crack. Bazant [1976] and Bazant and Cedolin [1979] used a smeared crack model to model cracking in concrete. In this model, the crack front is assumed to consist of a diffuse zone of microcracks and the stresses that close FPZ faces are represented through a stress-strain softening law.

Prasad and Krishnamoorthy [2002] developed a 2D computational model for investigation of crack formation and crack growth in plain and RC plane stress members. Attard and Tin-Loi [2005] conducted studies on numerical simulation of quasi-brittle fracture in concrete. Fracture was modeled through a constitutive softening–fracture law at the interface nodes, with the material within the triangular unit remaining linear elastic. Wu et al. [2006] proposed an analytical model to predict the effective fracture toughness of concrete based on the fictitious crack model. The equilibrium equations of forces in the section were derived in combination with the plane section assumption. Slowik et al. [2006] presented a method for determining tension softening curves of cementitious materials based on an evolutionary algorithm. Extensive research work was carried out by Raghu Prasad and Vidya Sagar [2006] towards numerical modelling of fracture and size effect in plain concrete using lattice mode. The concept of lattice model is discretization of the continuum by line elements such as bar and beam elements, which can transfer forces and moments. Roesler et al. [2007] developed a finite element based cohesive zone model using bilinear softening to predict the monotonic load versus crack mouth opening displacement of geometrically similar notched concrete specimens. The fracture parameters obtained based on the size effect method or the two-parameter fracture model, were found to adequately characterize the bilinear softening model. Xu and Zhang [2008] described double-G fracture model for concrete specimens based on strain energy release rate. This model couples the Griffith brittle fracture theory with the bridging softening property of concrete and it is an extension of double-K fracture model. It was observed that the results obtained from the double-G fracture model agree well with those of double-*K* fracture model. Kim et al. [2009] applied clustered discrete element method for the investigation of size effect on fracturing of asphalt concrete. Micromechanical fracture modelling approach was also carried out to investigate the heterogeneous fracture behaviour for different specimen sizes.

This paper presents methodologies for fracture analysis of concrete structural components with and without considering tension softening effect. SIF is obtained by using analytical approach and finite element analysis. In the analytical approach, SIF accounting for tension softening effect is obtained as the difference of SIF obtained using LEFM principles and SIF due to crack closing pressure. Superposition principle has been used for accounting the non-linearity in incremental form. SIF due to closing force applied on the effective crack face inside the process zone has been computed by using Green's function approach. In finite element analysis, the domain integral method has been used for computation of SIF. The domain integral method is used to calculate the strain energy release rate (SERR) when a crack grows and converts it to SIF by using the relations between stresses and energy. Numerical studies have been conducted on notched 3-point bending concrete specimen with and without considering the cohesive stresses. It is observed from the studies that SIF obtained from the finite element analysis with and without considering the cohesive stresses is in good agreement with the corresponding analytical value.

2 Concrete Fracture Models

Based on different energy dissipation mechanisms, nonlinear fracture mechanics (NLFM) models for quasi-brittle materials can be classified as a fictitious crack approach (cohesive crack model) and an equivalent-elastic crack approach. Fracture mechanics models using only the Dugdale-Barenblatt energy dissipation mechanism are usually referred to as the fictitious crack approach, whereas fracture mechanics models using only the Griffth-Irwin energy dissipation mechanism are usually referred to as the effective-elastic crack approach or equivalent-elastic crack approach.

The energy release rate for a mode I quasi-brittle crack, G_q, can be expressed as [Shah et al. (1995)].

$$G_q = G_{\mathrm{Ic}} + G_\sigma \tag{1}$$

where, G_{Ic}= Critical energy release rate

G_σ = Work done by the cohesive pressure over a unit length of crack

Brief description of fictitious crack model is presented below [Shah et al. (1995)].

2.1 Fictitious crack approach (Cohesive crack model)

The fictitious crack approach assumes that energy to create the new surface is small compared to that required to separate them, and the energy rate term G_{IC} vanishes in eqn. (1). Figure 2 shows the simulation of a newly formed crack structures and the corresponding fracture process zone [Shah et al. (1995)]. As a result, the energy dissipation for crack propagation can be completely characterized by the cohesive stress-separation relationship σ(w). Since all energy produced by the applied load is completely balanced by the cohesive pressure, eqn. (1) is reduced to (with G_{Ic} = 0).

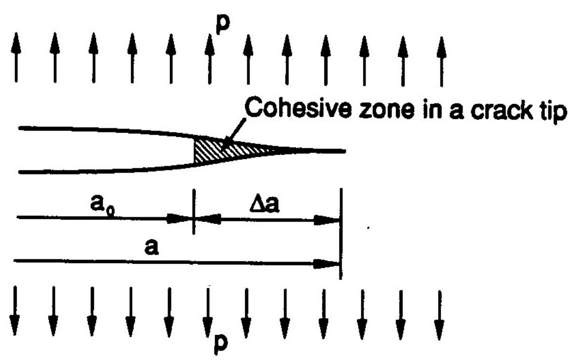

Figure 2: Mode I crack for fictitious crack approach

$$G_q = \int_0^{w_t} \sigma(w)\ \mathrm{dw} \tag{2}$$

Eqn. (2) is valid for structures with a constant thickness. The fictitious crack is assumed to initiate and propagate when the principal tensile stress reaches the tensile strength of material f_t.

Cohesive crack model requires a unique σ(w) curve to quantify the value of energy dissipation. The choice of the σ(w) function influences the prediction of the structural response significantly, and the local fracture behavior, for example the crack opening displacement, is particularly sensitive to the shape of σ(w). Many different σ(w) curves, including linear, bilinear, trilinear, exponential, and power functions, have been used in the literature [Shah et al. (1995)].

2.2 SIF computation

Prediction of the remaining life or residual strength of a fatigue-damaged structure depends on proper understanding of the crack growth behaviour, which in turn relies on the computation of SIF accurately. Fracture analysis has been carried out for concrete structural components with and without considering cohesive stresses. SIF has been computed by using analytical approach and finite element analysis.

2.2.1 Analytical approach

In this approach, one of the major assumptions is to use fracture mechanics principles to describe the crack growth phenomena during the acceleration stage of fatigue crack growth in concrete. The fatigue mechanism in plain concrete may be attributed to progressive bond deterioration between aggregates and matrix or by development of cracks existing in the concrete matrix. These two mechanisms may act together or separately, leading to complexity of the fatigue mechanism. It is well known fact that concrete typically exhibits nonlinear fracture processes because of the large FPZ, leading to LEFM based approach objectionable. Hence, an analytical model for assessing the fatigue life of concrete accounting for the tension softening effect is required. The following are the basic assumptions of tension softening.
Modelling assumptions

- Plane sections of the beam remain plane after deformation
- Fictitious crack surface remains plane after deformation
- Normal closing tractions acting on the fictitious crack follow the linear stress crack opening displacement
- Bending stress in the concrete along the bottom of the beam is equal to the traction normal to the crack mouth at the bottom of the beam.

Stress intensity factor (SIF) accounting for the tension softening effect has been obtained as difference of SIF obtained by using LEFM principles and SIF due to closing pressure. Principle of superposition has been used by accounting for the nonlinearity in incremental form. SIF due to the closing force applied on the effective crack face inside the process zone has been computed by using Green's function approach by employing appropriate softening relation. It is assumed that the crack opening displacement at any point will follow the linear relationship with the crack tip opening displacement (CTOD) and crack depth for each crack increment (Δa). Further, CTOD is a function of crack mouth opening displacement and the associated geometry factor. Various tension softening models such as linear, bi-linear, tri-linear, exponential and power curve have been used to represent the tension softening effect.

The details of the model are given below:

To incorporate the tension softening behaviour, based on the principle of superposition, SIF has to be modified as shown in Figure 3.

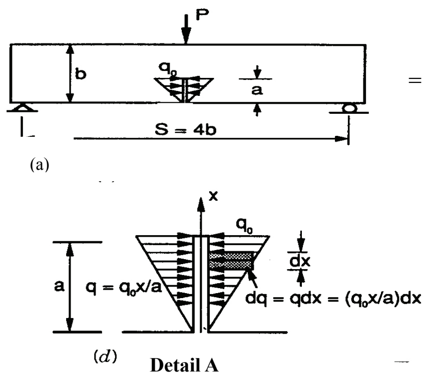

Figure 3: Illustration of superposition principle

$$K_I = K_I^P - K_I^q \tag{3}$$

where K_I^P is SIF for the concentrated load P in a three point bending beam, and K_I^q is SIF due to the closing force applied on the effective crack face inside the process zone, which can be obtained through Green's function approach by knowing the appropriate softening relation. Superposition principle is used by accounting for the non- linearity in incremental form.

Computation of K_I^P

SIF due to the concentrated load P can be calculated by using LEFM principles. For the three-point bending beam shown in Figure 3b, SIF can be expressed as

$$K_I^p = \sigma\sqrt{\pi a}g_1\left(\frac{a}{b}\right) \text{ where, } \sigma = \frac{3\text{PS}}{2\text{b}^2\text{t}} \tag{4}$$

where P= applied load, a= crack length, b= depth of the beam, t= thickness and

g_1(a/b)= geometry factor, depends on the ratio of span to depth of the beam and is given below for S/b=2.5 [Tada et al. (1985)].

$$g_1\left(\frac{a}{b}\right) = \frac{1.0 - 2.5a/b + 4.49(a/b)^2 - 3.98(a/b)^3 + 1.33(a/b)^4}{(1 - a/b)^{3/2}} \tag{5}$$

For S/b=4.0;

$$g_1\left(\frac{a}{b}\right) = \frac{1.99-(a/b)+(1-a/b)\left[2.15-3.93(a/b)+2.7(a/b)^2\right]}{\sqrt{\pi(1+2a/b)}\,(1-a/b)^{3/2}} \tag{6}$$

For S/b=8.0;

$$g_1\left(\frac{a}{b}\right) = 1.11-1.55(a/b)+7.71(a/b)^2-13.55(a/b)^3+14.25(a/b)^4 \tag{7}$$

Computation of K_I^q

The incremental SIF due to the closing force dq can be expressed as [Shah et al. (1995)].

$$dK_I^q = \frac{2}{\sqrt{\pi\Delta a}}dq\, g\left(\frac{a}{b},\frac{x}{a}\right) \tag{8}$$

where dq can be expressed as function of softening stress distribution over the crack length Δa; the function 'g' represents the geometry factor.

Calculation of 'dq'

By using the above concept (Figure 3d), cohesive crack can be modelled in the following manner (Figure 4).

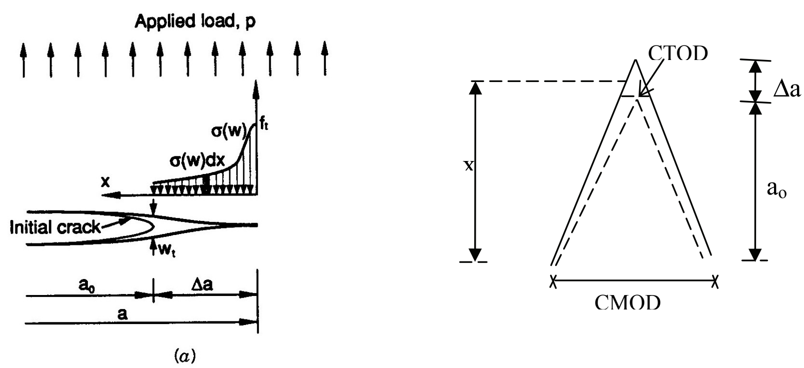

(a) Modelling of quasi-brittle crack with crack surfaces in contact

(b) Schematic diagram of crack Opening displacement

Figure 4: Cohesive crack modelling

The crack opening displacement w at any point x is assumed to follow linear relationship (Figure 4) and can be expressed as,

$$w = \delta\left(\frac{a_0 - x}{\Delta a} + 1\right) \quad a_0 \leq x \leq a_{eff} \tag{9}$$

where δ is the crack tip opening displacement and a_0 is the initial crack length.
As an example, consider linear softening law

$$\sigma = f_t\left(1 - w/w_c\right) \tag{10}$$

where f_t = tensile strength of concrete and w_c=critical crack opening displacement
Substituting for w from eqn. (9) in the linear softening law given by eqn. (10), one can obtain,

$$dq = \sigma = f_t\left\{1 - \frac{\delta}{w_c}\left(\frac{a_0 - x}{\Delta a} + 1\right)\right\}dx \tag{11}$$

The crack opening displacement at any point δ(x) can be calculated by using,

$$\delta(x) = CMODg_3\left(\frac{a}{b}, \frac{x}{a}\right) \tag{12}$$

where

$$g_3\left(\frac{a}{b}, \frac{x}{a}\right) = \left\{\left(1 - \frac{x}{a}\right)^2 + \left(1.081 - 1.149\frac{a}{b}\right)\left[\frac{x}{a} - \left(\frac{x}{a}\right)^2\right]\right\}^{1/2} \tag{13}$$

where CMOD is crack mouth opening displacement and is calculated by using,

$$CMOD = \frac{4\sigma a}{E}g_2\left(\frac{a}{b}\right) \tag{14}$$

where g_2(a/b) is geometric factor, which depends on the ratio of span to depth of the beam and is given below for S = 2.5b

$$g_2(a/b) = \frac{1.73 - 8.56a/b + 31.2(a/b)^2 - 46.3(a/b)^3 + 25.1(a/b)^4}{(1 - a/b)^{3/2}} \tag{15}$$

Hence, replacing dq in eqn. (8) and integrating over length Δa, K_I^q can be obtained as,

$$K_I^q = \int_{a_0}^{a_{eff}} \frac{2f_t}{\sqrt{\pi\Delta a}}\left\{1 - \frac{\delta}{w_c}\left(\frac{a_0 - x}{\Delta a} + 1\right)\right\}g\left(\frac{a}{b}, \frac{x}{a}\right)dx \tag{16}$$

where

$$g\left(\frac{a}{b},\frac{x}{a}\right)=\frac{3.52(1-x/a)}{(1-a/b)^{3/2}}-\frac{4.35-5.28x/a}{(1-a/b)^{1/2}} + \left[\frac{1.30-0.30(x/a)^{3/2}}{\sqrt{1-(x/a)^2}}+0.83-1.76\frac{x}{a}\right]\left[1-\left(1-\frac{x}{a}\right)\frac{a}{b}\right] \tag{17}$$

Similar expressions can be obtained for other models such as bilinear, trilinear, exponential, power law etc.

After evaluating K_I^P using eqn. (4) and K_I^q using eqn. (16), K_I can be calculated by using eqn. (3).

2.2.2 Finite Element Analysis

Finite element analysis (FEA) has been carried out using the general purpose software, ABAQUS. The domain integral method is used to calculate strain energy release rate (SERR) when a crack grows and to compute SIF by assuming plane stress/ strain conditions. The details of the method are given below.

The energy domain integral (Shih et al, 1986)

For stable crack growth in a two-dimensional body having a line crack along the x_1 axis, SERR per unit crack growth is,

$$J=\lim_{\Gamma\to 0}\int_{\Gamma}\left(W\delta_{1i}-\sigma_{ij}u_{j,1}\right)n_i dC \tag{18}$$

where W is the stress work density, σ_{ij} and u_i are components of the stress and displacement along the x_i axis, $n_i$is the unit vector normal to Γ contour and dC is the infinitesimal arc length as depicted in Figure 5.

In the absence of thermal strain, body force, crack face traction and by applying the divergence theorem to eqn. (18),

$$J=\int_{A}\left[\left(\sigma_{ij}u_{j,1}-W\delta_{1\tau}\right)q_1\right]dA \tag{19}$$

where A is the area enclosed by C. Invoking the equilibrium equation, the domain expression for SERR is,

$$J=\int_{A}\left[\sigma_{ij}u_{j,1}-W\delta_{1i}\right]q_{1,j}dA \tag{20}$$

The function q_1 can be interpreted as a unit translation on Γ in the $x_1$direction while keeping the material points on C_1 fixed. According to the vanishing of Γ around the tip, this can be viewed as the growing of the crack.

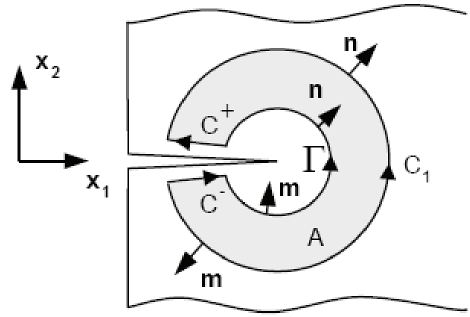

Figure 5: Closed contour $C = C_1 - \Gamma + C^+ + C^-$ enclosing a simply connected region A

Finite element formulation for the domain integral method

For the six-node isoparametric element, the coordinates, displacements, and a smooth function are,

$$x_i = \sum_{k=1}^{6} N_k X_{ik} \tag{21}$$

$$u_i = \sum_{k=1}^{6} N_k U_{ik} \tag{22}$$

$$q_1 = \sum_{k=1}^{6} N_k Q_{1k} \tag{23}$$

where N_k are the shape functions, X_{ik} are the nodal coordinates, U_{ik} are the nodal displacements and Q_{1k} are the nodal values of the smooth function varying between 1 and 0.

For 2x2 Gaussian integration, SERR expression is,

$$J = \sum_{\text{all elements in } A} \sum_{p=1}^{4} W_p \left\{ \left[\sigma_{ij} \frac{\partial u_j}{\partial x_1} - W \delta_{1i} \right] \frac{\partial q_1}{\partial x_1} \det \left(\frac{\partial x_k}{\partial \eta_k} \right) \right\}_p t \tag{24}$$

where all quantities are calculated at the 4 Gauss points with W_p as their respective weights and t is the specimen thickness.

3 Numerical Studies

Numerical studies have been carried out on fracture analysis of concrete structural components with and without considering cohesive stresses in the analysis. Two example problems are presented herein.

Problem-1: This problem was experimentally studied by Toumi, et al. [1998]. The details of the problem are shown below (Figure 6).

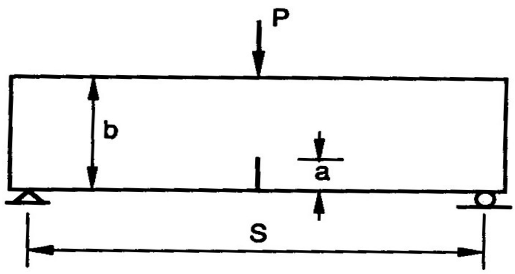

Figure 6: Geometry of 3 point bending specimen

Span(S) =320mm, Depth (b) =80mm, Thickness (t) =50mm, Initial crack length=4mm, Load =750N, Modulus of elasticity=37750 MPa, Tensile strength=4.2 MPa, S/b=4.

Fracture analysis has been carried out for several crack lengths. SIF has been evaluated with and without considering cohesive stresses in the analysis.

Figure 7 shows FE mesh, loading, cohesive stresses and boundary conditions. Cohesive stresses have been defined as described in analytical section 2.2(a). Eight noded solid elements have been employed for FE modelling of the beam.

Figure 8 shows the von Mises stress contour along with zoomed view, without considering the cohesive stresses in the FE analysis.

Figure 9 shows the von Mises stress contour by considering cohesive stress in the analysis along with zoomed view.

Figure 10 shows the FE mesh and characteristics for a crack length of 40mm including zoomed view of cohesive stresses. Further, the von-Mises stress contour corresponding to crack length of 40mm by considering cohesive stress along with the zoomed view of crack front is shown in Figure 11.

Table 1 shows the SIF values of both analytical and FEA with and without considering cohesive stress for different crack lengths.

It can be observed from Table 1 that computed values of SIF from FE analysis are in very good agreement with the corresponding analytical SIF values for both cases.

Table 1: SIF values for different crack lengths with and without cohesive stresses (Load = 750 N)

Crack Length, mm	SIF, MPa $\sqrt{m}$				%difference in SIF with & and without cohesive (FEA)
	Analytical		FEA		
	without cohesive	with cohesive	without cohesive	with cohesive	
4	3.881	3.381	3.748	3.219	14.11
8	5.2437	4.79	5.149	4.609	10.48
12	6.28	5.67	6.087	5.557	8.70
16	7.24	6.721	7.194	6.656	7.47
20	8.217	8.01	8.535	7.982	6.47
24	9.295	8.95	9.318	8.776	5.82
28	10.39	9.78	10.13	9.588	5.35
32	12.07	11.67	12.01	11.46	4.58
36	13.96	13.21	13.47	12.93	4.00
40	16.33	15.64	15.89	15.37	3.27

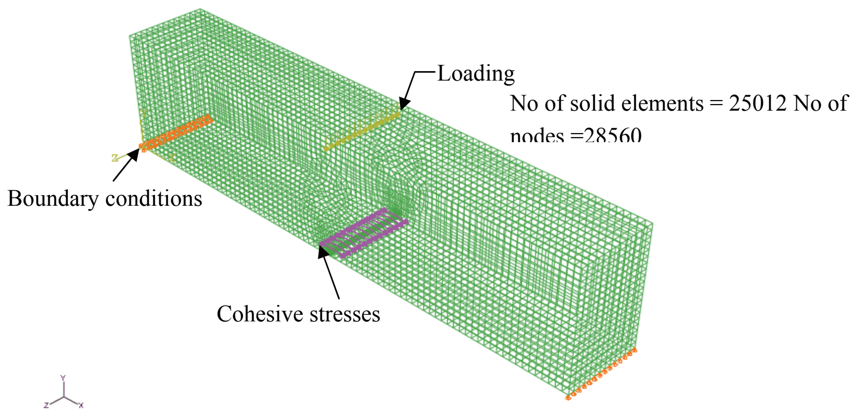

Figure 7: FE mesh (crack length=4mm)

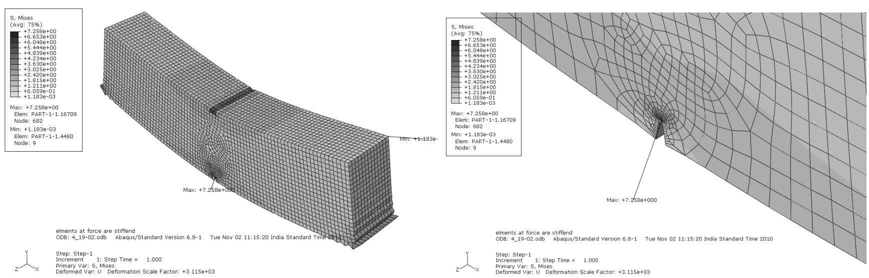

Zoomed view of crack front stresses

Figure 8: von-Mises stress contour without cohesive stress

Figure 12 shows the plot of SIF values with and without cohesive stresses for various crack lengths.

From Table 1 and Figure 12, it can be observed that the effect of cohesive stresses on SIF decreases with increase of crack length and is significant for larger crack lengths. Further parametric studies have been carried out on SIF by varying the parameters such as load, crack length and tensile strength.

Problem-2: This problem was experimentally studied by Bazant and Schell [1993]. The details of the problem are presented below. Different beam lengths and depths were considered for analysis to investigate the size effect.

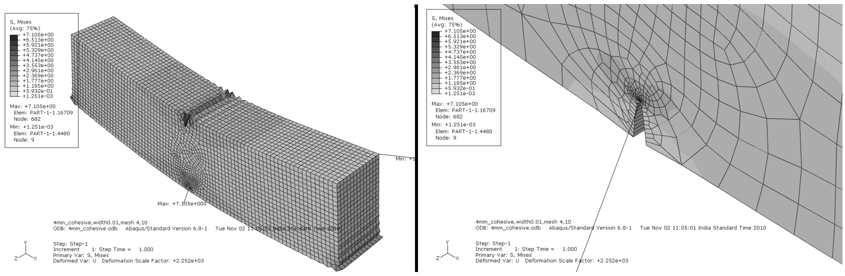

Zoomed view of crack front stresses

Figure 9: von Mises stress contour with cohesive stress

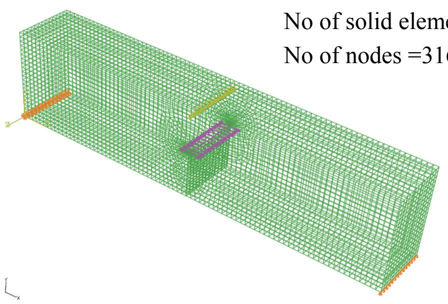

No of solid elements = 27807
No of nodes =31640

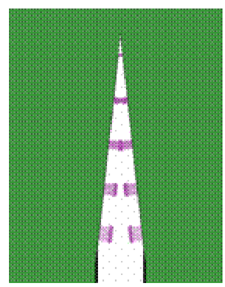

Zoomed view of cohesive stresses

Figure 10: FE mesh (crack length=40mm)

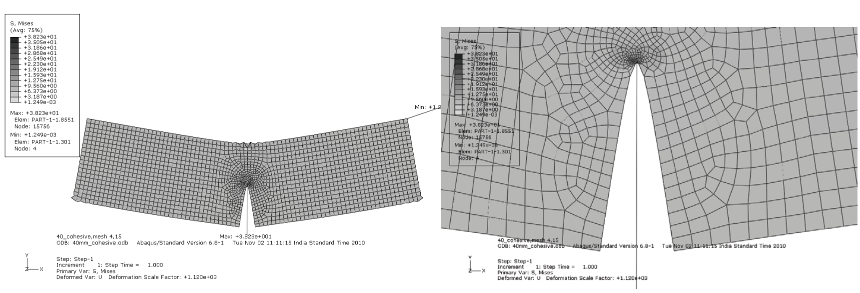

Zoomed view of crack front stresses

Figure 11: von-Mises stress contour with cohesive stress (crack length=40mm)

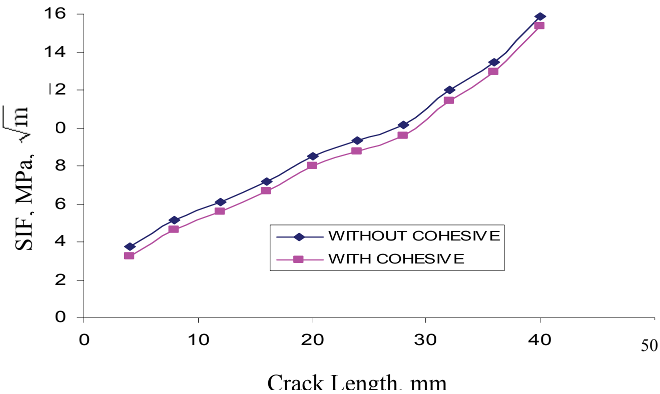

Figure 12: Crack length vs SIF

Beam depth (b)=38.1, 107.8, 304.8 mm

Span (S) =2.5 * beam depth, Thickness (t) =38.1 mm

Initial crack length =b/6 mm, Modulus of elasticity =38,300 MPa

Tensile strength =8.9 MPa

Fracture analysis has been carried out for several crack lengths. SIF has been evaluated with and without considering cohesive stresses in the analysis. SIF without and with cohesive stresses for different crack lengths are shown in Figure 13. From Fig 13, it can be observed that the effect of cohesive stresses on SIF decreases with increase of crack length and is significant (about 23%) for larger crack lengths. From Figure 13, it can also be observed that there is significant effect (as high as 65%) of cohesive stress on SIF for larger beam depth and span.

Figure 14 shows the variation of SIF with load for various dimensions of the beam. From Figure 14, it can also be observed that the effect of cohesive stress on SIF is less with increase of load and crack length in the case of geometrically similar structures. Figure 15 shows the variation of SIF with tensile strength for various crack lengths and beams. In general, it can be observed that SIF values are decreasing with increase of tensile strength for a particular crack length.

4 Summary and Concluding Remarks

Analytical methodologies for SIF computation of concrete structural components considering the tension softening have been presented. SIF accounting for tension softening effect is calculated as difference of SIF obtained using LEFM principles and SIF due to closing pressure. Superposition principle has been used by

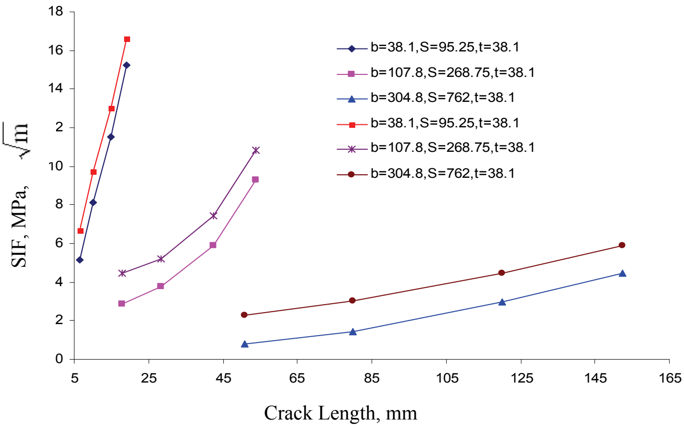

Figure 13: Crack length vs SIF for geometrically similar components

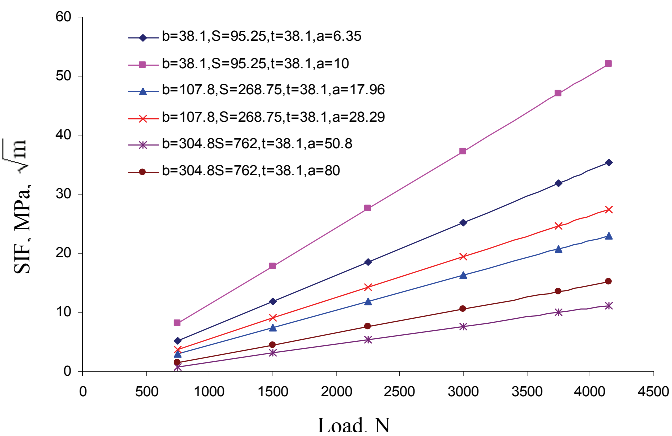

Figure 14: Load vs SIF for geometrically similar components

accounting for the non-linearity in incremental form. SIF due to closing force applied on the effective crack face inside FPZ has been computed by using Green's function approach. The domain integral method has been used for computation of SIF. The domain integral method is used to calculate SERR and SIF when a crack grows. Numerical studies have been conducted on 3-point bending concrete specimen with and without considering the cohesive stresses. It is observed from the studies that SIF obtained from the finite element analysis with and without considering the cohesive stresses is in good agreement with the corresponding analytical

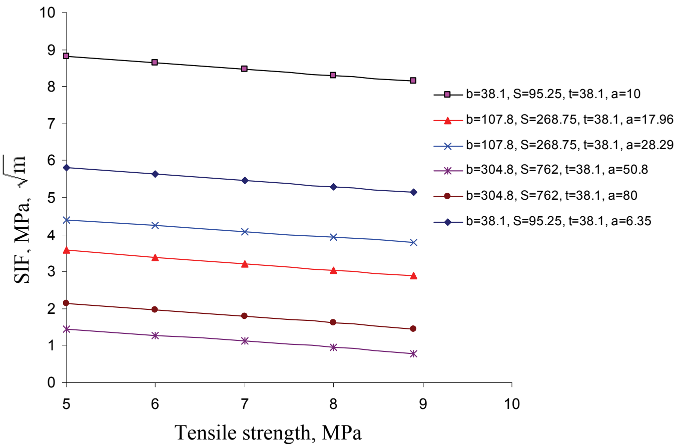

Figure 15: Tensile strength vs SIF for geometrically similar components

value. Further, parametric study on SIF has been carried out by varying the load, crack length and tensile strength for geometrically similar structures. From the studies, it is observed that the effect of cohesive stress on SIF

- decreases with increase of crack length and is significant for larger crack lengths keeping load as constant
- is lesser with increase of load for a particular crack length and is significant for larger loads
- decreases with increase of tensile strength for a particular crack length and load

Acknowledgement: We acknowledge with thanks the valuable technical suggestions and support provided by our colleague Mr J. Rajasankar, Deputy Director for useful technical discussions during the course of this investigation. This paper is being published with the permission of the Director, CSIR, SERC, Chennai, India.

References

Anderson, T.L. (1995): *Fracture mechanics: fundamentals and applications*, CRC Press.

Attard, M. M.; Tin-Loi, F. (2005): Numerical simulation of quasi-brittle fracture in concrete. *Engg. Fract. Mech.*, vol. 72, no. 3, pp. 387-411.

Barenblatt, G.I. (1959): Equilibrium cracks formed during brittle fracture. *Prikl Mat Mech*, vol.**23**.

Bazant Z.P.; Schell W F. (1993): Fatigue Fracture of High strength concrete and size effect. *ACI materials J.,* vol. 90, no. 5, pp. 472-478.

Bazant, Z.P. (1976): Instability, ductility and size effect in strain-softening concrete. *J. Engg. Mech., ASCE*, vol. 102, pp. 331-344.

Bazant, Z.P. (2002): Concrete fracture model: testing and practice. *Engg. Fract. Mech.*, vol. 69, pp. 165-205.

Bazant, Z.P.; Cedolin, L. (1979): Blunt crack bond propagation in finite element analysis. *J. Engg. Mech., ASCE*, vol. 105, no. 2, pp. 297-315.

Dugdale, D.S. (1960): Yielding of steel sheets containing slits. *J. Mech. Physics of Solids*, vol. **8**.

Hillerborg, A.; Modeer, M.; Petersson, P.E. (1976): Analysis of crack formation and crack growth in concrete by means of fracture mechanics and finite elements. *Cement and concrete research*, vol. 6, pp. 773-782.

Kaplan, M.E. (1961): Crack propagation and fracture of concrete. *J. American Concrete Institute*, vol. 58(5), pp. 591-610.

Kim H. Wagoner, Mi. P.; Buttlar, W G. (2009): Numerical fracture analysis on the specimen size dependency of asphalt concrete using a cohesive softening model. *Construct. Building Mater.*, vol. 23(5), pp. 2112-2120.

Prasad, M.V.K.V.; Krishnamoorthy, C.S. (2002): Computational model for discrete crack growth in plain and reinforced concrete. *Comput. Methods Appl. Mech. Engg.,* vol. 191, pp. 2699–2725.

Raghu Prasad, B.K.; Vidya Sagar, R. (2006): Numerical modelling of fracture and size effect in plain concrete. *J. Institution of Engineers (India)*, vol. 86, pp. 182-186.

Roesler, J.; Paulino, G. l H.; Park K; Gaedicke, Cristian, (2007): Concrete fracture prediction using bilinear softening. *Cement and Concrete Composites*, vol. 29, 4, pp. 300-312.

Shah, S.P.; Swartz, S.E.; Ouyang, C. (1995): *Fracture Mechanics of Concrete: Applications of Fracture Mechanics to Concrete, Rock and other Quasi-brittle Material,* John Wiely Sons, Inc, New York.

Shih, C.F.; Moran, B.; Nakamura, T. (1986): Energy Release Rate along a Three - dimensional Crack Front in a Thermally Stressed Body. *Int. J. Fract.,* vol. 30, pp. pp. 79- 102.

Slowik, V.; Beate Villmann B.; Bretschneider N.; Villmann, T. (2006): Computational aspects of inverse analyses for determining softening curves of concrete. *Comput. Methods Appl. Mech. Engg.*, vol. 195, pp. 7223–7236.

Subramaniam, V.K.; Neil, E.F.; Popovics, S.J.; and Shah, S.P. (2000): Crack propagation in flexural fatigue of concrete. *J. Engg. Mech.*, *ASCE*, vol. 126(9), pp. 891-898.

Tada, H.; Paris, P.C.; Irwin, G.R. (1985): *The Stress Analysis of Cracks Handbook.* 2^{nd} ed., *Paris Productions, St. Louis, MO.*

Toumi, A.; Turatsinze, A. (1998): Crack propagation in concrete subjected to flexural cyclic loading. *Mater. Struct.*, vol. 31, pp. 451-458.

Wu, Z.; Yang, S.; Hu, X.; Zheng, J. (2006): An analytical model to predict the effective fracture toughness of concrete for three-point bending notched beams. *Engg. Fract. Mech..*, vol. 73(15), pp. 2166-2191.

Xu, S.; Zhang, Xi. (2008): Determination of fracture parameters for crack propagation in concrete using an energy approach. *Engg. Fract. Mech.*, vol. 75, 15, pp. 4292-4308.